Journal of Catalysis **199,** 291–301 (2001)
doi:10.1006/jcat.2001.3176, available online at http://www.idealibrary.com on IDEAL®

Turnover Rate and Reaction Orders for the Complete Oxidation of Methane on a Palladium Foil in Excess Dioxygen

R. S. Monteiro,* D. Zemlyanov,* J. M. Storey,† and F. H. Ribeiro*,[1]

*Worcester Polytechnic Institute, Department of Chemical Engineering, Worcester, Massachusetts 01609-2280; and †Oak Ridge National Laboratory, P.O. Box 2009, MS 8087, Oak Ridge, Tennessee 37831-8087

Received September 14, 2000; revised January 17, 2001; accepted January 18, 2001

The turnover rate and reaction orders for the combustion of methane in excess oxygen over Pd foils were in agreement with literature results reported for supported catalysts. The rate equation was $r = k[CH_4]^{0.7}[O_2]^{0.2}[H_2O]^{-0.9}$. The turnover rate on the Pd foil was 59×10^{-2} s^{-1} at 550 K, 160 Torr O_2, 16 Torr CH_4, 1 Torr H_2O, and N_2 balance to 800 Torr, with the number of active sites defined as the number of surface Pd atoms calculated from the initial geometric area of the foil. This rate is 3 times higher than the highest value reported in the literature for supported catalysts. The surface area of the foil, measured by isotopic exchange of surface oxygen with $^{18}O_2$, increased by a factor of approximately 2 after reaction. The main species observed on the surface after reaction by XPS was PdO. Sample activation during the reaction was not observed. The reaction was carried out in a batch reactor at 598 K and atmospheric pressure with characterization before and after reaction by X-ray and Auger spectroscopies and temperature-programmed desorption.

Key Words: **palladium foil; palladium oxide; turnover rate for methane combustion; reaction orders for methane combustion; model catalysts.**

1. INTRODUCTION

Catalytic combustion of CH_4 is an environmentally friendly alternative to conventional thermal combustion in gas-fired turbines for power generation. Turbines with conventional burners produce substantial amounts of NO_x while catalytic combustion has the potential to lower nitrogen oxide emissions below 1 ppm. Current turbines need only the energy provided by the adiabatic combustion of a lean mixture, and currently can use final temperatures of the order of 1300°C. At this temperature and with residence times typical of a turbine, there should be NO_x levels much below 1 ppm. However, these lean mixtures do not allow a conventional burner to function properly and for this reason more fuel is added to the mixture to stabilize the combustion, generating unnecessarily high temperatures which form undesirable NO_x. In catalytic combustion, the role of the catalyst is to assist the combustion of lean premixed mixtures by preheating them to a high enough temperature to allow the reaction mixture to proceed to complete combustion downstream in the homogeneous phase (1).

Global warming caused by emissions of methane is also a concern if there will be a widespread adoption of natural-gas-powered vehicles. Catalytic combustion can be used as an abatement technology to eliminate unburned methane.

Palladium shows the highest turnover rate for this reaction (2) but more active materials are still needed for combustion at the high values of mass throughput found in gas turbine operation (3). Palladium oxide (PdO) is the stable phase under reaction conditions with excess oxygen (>1073 K, in 1 atm air) (4, 5). Its reactivity has been linked to particle size (6–8), support interaction (9), crystal structure (10, 11), and reaction conditions (12, 13). Activation periods have also been reported during CH_4 combustion. It is well known that some activation periods observed were due to elimination of contaminants, which interacted with metallic sites (14, 15). However, changes in the morphology with reconstruction of the palladium crystallites were also assigned to explain time-on-stream activation on catalysts with no contaminants (16–18). The consequence of all of these unknowns is that rates of reaction reported in the literature span a range of 4 orders of magnitude. Clearly, the rate of oxidation must be measured and the parameters that are important in modifying the rates need to be identified.

The approach for the present work was to use a model system to study particular aspects of the catalytic combustion chemistry of methane on Pd catalysts. The advantage of this approach is that one can apply surface science techniques and yet carry out reactions under the conditions described in the literature for supported catalysts, a method pioneered by G. A. Somorjai (see (19) for a review). Because they include control of sample purity and detailed surface analysis before and after reaction, these studies should provide the benchmark kinetic measurements for comparison with supported catalysts.

[1] To whom correspondence should be addressed. Fax: 508-831-5853. E-mail: fabio@wpi.edu.

0021-9517/01 $35.00

The kinetic behavior was in agreement with the kinetics found in supported samples, with the following rate expression: $r = k[CH_4]^{0.7}[O_2]^{0.2}[H_2O]^{-0.9}$ (20–23). The turnover rate for the Pd foil based on the number of surface Pd atoms (calculated using the geometric surface area of the foil) was 3 times higher than the highest rate reported for supported catalysts, which is possibly the maximum rate that can be achieved on a Pd catalyst. One problem, however, is that PdO and not Pd is the active phase and there are indications in the literature (12, 13, 20, 24) that upon oxidation the surface area of the oxide will be higher than the surface area of the metal. Throughout the literature on supported Pd catalysts, the reported turnover rates are based on the number of Pd sites counted in the reduced state of the catalysts. In our case, we used the geometric surface area to calculate the amount of active sites for direct comparison with the literature but we also measured the PdO surface area by ^{18}O isotope exchange. The results showed that the Pd foil surface area is increased by a factor of about 2 after reaction.

Despite reports of activation periods in supported samples in the literature (16–18, 20), the Pd foil did not show any activation under reaction conditions. However, for the Pd foils in this work steady-state activities were reached only after elimination of all surface impurities, as verified by X-ray and Auger spectroscopies.

2. EXPERIMENTAL METHODS

The combustion of methane at atmospheric pressure was performed on a batch reactor attached to an ultrahigh-vacuum (UHV) surface analysis chamber. Sample transfer between the two chambers was made with a welded bellows transfer arm under UHV. The ultimate pressure after baking out the system was 5×10^{-10} Torr (1 Torr = 133.3 N m^{-2}). The main components of the analysis chamber are a double-pass cylindrical mirror analyzer (PHI Model 15-255G) used for Auger electron spectroscopy (AES) and X-ray photoelectron spectroscopy (XPS), a 15 kV double-anode X-ray gun (PHI 4-548), a UTI-100C quadrupole mass spectrometer, and a sputtering gun. The sample was spot-welded between two stainless steel pins attached to a Macor sample holder. The sample temperature was measured by using a chromel–alumel thermocouple spot-welded directly onto the palladium foil. The sample cart holder inside the UHV chamber could be rotated to the various analysis stations. The sample was heated resistively and the temperature was controlled by using an Eurotherm 2408 controller interfaced with a TCR DC power supply.

The palladium catalysts were 0.1-mm-thick polycrystalline foils (Alfa Aesar, 99.9%) with a surface area of 0.8–1.0 cm^2. The cleaning procedure consisted of sputtering with 2.0 kV Ar ions (15 μA ion current) at 773 K for 15 min, exposure to O_2 (5×10^{-5} Torr of O_2) at 773 K for 15 min, followed by annealing at 873 K for 60 s under UHV conditions. After the initial cleaning sequence (sputtering/O_2 treatment/annealing), the sample deactivated under methane combustion with silicon and phosphorous detected by XPS. The sample reached steady-state rates only after it was subjected to many methane combustion reaction experiments at high pressure in addition to the sputtering/annealing treatment. The contaminants on a fresh foil were carbon, phosphorus, silicon, and sulfur. Sample cleanliness was checked by AES and XPS analyses. Auger spectra were obtained with a primary beam voltage of 2 kV and a beam current of 2 μA. X-ray photoelectron spectroscopy was performed using Mg$K\alpha$ (1253.6 eV) or A1$K\alpha$ (1486.6 eV) radiation at a power of 300 W. Survey spectra on XPS were recorded using an analyzer pass energy of 100 eV, whereas on the core level measurements for Pd 3*d*, O 1*s*, and C 1*s* the analyzer pass energy was 25 eV. The resolution measured at full width at half-maximum (FWHM) for the Pd $3d_{5/2}$ peak was 1.2 eV.

The sample was moved from the UHV chamber to the reactor cell using a welded bellows transfer arm. Reactions were carried out in a batch mode with the gases being introduced from the manifold in the following order: N_2 (624 Torr), O_2 (160 Torr), and finally CH_4 (16 Torr). The reaction mixture was circulated by a Metal Bellows pump Model MB-21 at a nominal rate of 1000 cm^3 min^{-1} for 25 min before the foil was heated to the reaction temperature (598 K). The total volume of the reactor cell as measured from expansion of a calibrated volume was 840 cm^3. There were dead volume pockets in the reactor but diffusion combined with low rates of product formation was sufficient to mix all the reactants and products. The gas phase composition was analyzed by using a HP 6890 series gas chromatograph equipped with a 15-ft Carboxen 1000, 60/80 mesh column, and a thermal conductivity detector. Sampling (every 18 min) was performed with an automatic sampling valve and the signal was acquired by a computer using HP ChemStation software. After reaction the sample was transferred back using the welded bellows transfer arm into the UHV chamber for surface analysis by XPS, AES, and TPD without exposure of the sample to the atmosphere. The TPD analysis consisted of heating the sample under UHV conditions to 873 K at a heating rate of 5 K s^{-1}. Desorption products were monitored by using a UTI-100C quadrupole mass spectometer (MS) and were recorded using a homemade acquisition software that runs under LabView.

Calibration of the MS was made after each TPD experiment by leaking O_2 into the system through a leak valve and using this signal to calculate all the other intensities. The CO_2 and H_2O signals were calibrated as a function of the O_2 signal by mixtures of CO_2–O_2 or H_2O–O_2. The absolute calibration of oxygen coverage was made by adsorbing oxygen at room temperature and assuming 0.25 monolayer

(ML) coverage after exposure of the foil to 7.5×10^{-6} Torr of O_2 for 20 min (25, 26). However, due to the high CO signal background in our UHV chamber, the adsorbed oxygen reacted with CO to form CO_2 before it could desorb as O_2. To eliminate possible artifacts in this procedure, we used labeled oxygen ($^{18}O_2$).

Palladium black (Alfa Aesar, 99.9%) was used as a reference. The sample had a BET surface area of 47 $m^2\,g^{-1}$ with a calculated mean particle size of 13.4 nm. Methane combustion was carried out at atmospheric pressure in a glass continuously stirred tank reactor (CSTR) with the catalyst supported on a fritted disk within the reactor and a thermocouple well in contact with the catalyst for precise catalyst temperature measurement. Reaction gases (0.1% CH_4, 2% O_2, 0.4% H_2O, and balance He to atmospheric pressure) were delivered into the system by mass flow controllers (Porter Instrument Co.). Water was added by passing helium through water in a saturator kept at 273 K. The reaction mixture was circulated with a Metal Bellows pump Model MB-21 at a flow rate of about 1000 $cm^3\,min^{-1}$. The flow rate into the CSTR circuit from the gas delivery portion of the system was about 40 $cm^3\,min^{-1}$. The reaction was carried out at 473 K.

3. RESULTS

3.1. Blank Experiments

Because the surface area of the catalyst is small ($\sim$1 cm^2), two experiments were performed to measure the background activity of the catalytic reactor. In the first experiment a stainless steel foil was used in place of the Pd foil under standard reaction conditions. Based on the limit of detection of our gas chromatograph, the background rate is lower than $1 \times 10^{-5}\,s^{-1}$ compared to the steady-state activity of $59 \times 10^{-2}\,s^{-1}$ under standard conditions (16 Torr CH_4, 160 Torr O_2, 1 Torr H_2O, N_2 balance to 800 Torr, and 598 K). In a second experiment, Pd foil was used in the reaction at standard conditions without cleaning. The initial reaction rate was $6 \times 10^{-2}\,s^{-1}$ under standard conditions, but decreased to zero after about 30 min of reaction, due to the migration of impurities to the surface. This experiment simulates the contribution of the back of the foil, which cannot be cleaned by sputtering, and at steady state is expected to be negligible.

3.2. Rate Measurements

The rate measurements were made in a batch reactor at a total final conversion of less than 10%. Under these conditions the rate should follow pseudo-zero-order kinetics and thus an accumulation plot (conversion versus time) would produce a straight line. However, the plot in Fig. 1A shows a curvature due to either deactivation or inhibition by one of the reaction products. A negative first-order dependence on water concentration has been reported before on supported Pd catalysts (20). In this study, the reaction order in H_2O was -0.9 (details below) and product inhibition can explain the curvature on the line. Assuming a water inhibition of -1, the reaction rate will be $r = -A/\chi$, where χ is the conversion (or the number of turnovers) and A depends upon the concentration of the reactants which are essentially constant at low conversion. Using this rate expression, the equation for the batch reactor will then be $d\chi/dt = B/\chi$, where t is time and B is a constant. The integration of this equation has a linear dependence between the square of conversion (or the number of turnovers) and

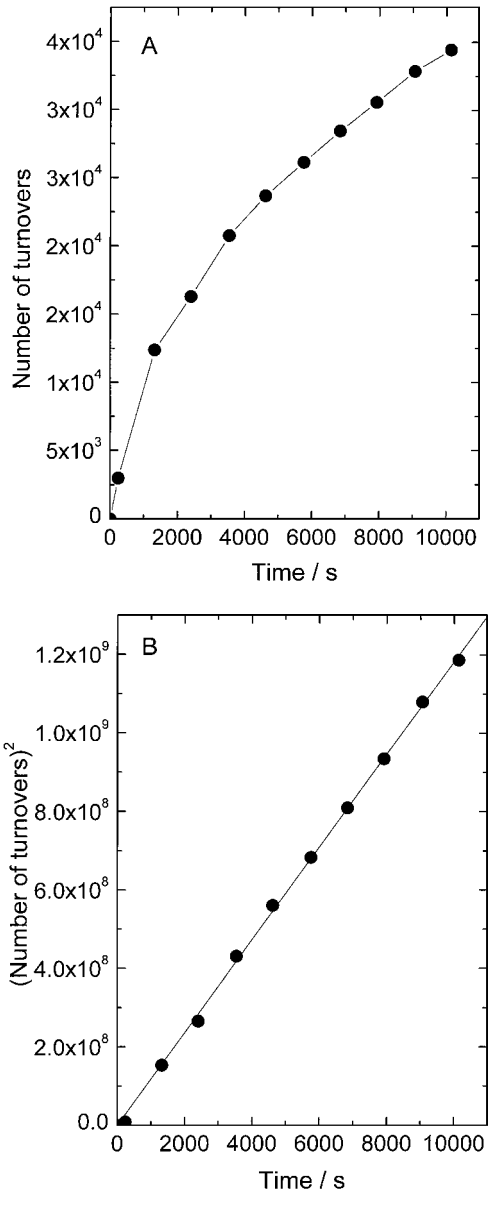

FIG. 1. (A) Batch reactor accumulation plot for Pd foil and (B) integrated form (accounted for H_2O inhibition). Reaction at 598 K, 16 Torr CH_4, 160 Torr O_2, and N_2 balance to 800 Torr.

TABLE 1

Kinetic Data for CH_4 Catalytic Combustion

Sample	E_a (kJ/mol)	TOR[a] (10^{-2} s^{-1})	Reaction dependence order			Reference
			CH_4	O_2	H_2O	
Pd foil	125	59	0.7	0.2	−0.9	This work
Pd black	135	5[b]	0.7	0.1	−0.8	This work
0.9–5% Pd/ZrO_2	184	3–18	1.1	0.1	−1.0	22
10% Pd/ZrO_2	170	2	—	—	−1.0	20

[a] TOR calculated at 550 K, 160 Torr O_2, 16 Torr CH_4, 1 Torr H_2O, and N_2 balance to 800 Torr.

[b] Number of sites measured from BET surface area (47 m^2 g^{-1}).

time ($\chi^2 = 2Bt$), and it is plotted in Fig. 1B. The slope of the line ($2B$) can then be used in the equation of the batch reactor to calculate the rate at any conversion. Therefore, the turnover rate is a function of the amount of water, and consequently the degree of conversion, and needs to be specified whenever a rate is reported. The turnover rates will be reported under the standard conditions of 1 Torr H_2O, 550 K, 16 Torr CH_4, and 160 Torr O_2 throughout this paper.

The turnover rate obtained for the Pd foil was 59×10^{-2} s^{-1} under standard conditions, a value higher than the ones observed for the ZrO_2-supported Pd and Pd black samples shown in Table 1. No activation period or deactivation of the samples was ever observed. Foils preoxidized in O_2 at the same partial pressure and temperature used for the reaction showed the same rate values as initially clean foils.

The reaction order dependence on CH_4, O_2, and H_2O was determined at 598 K. The results are shown in Fig. 2. Under these conditions, the catalytic combustion of methane on Pd foils is close to first order in CH_4, zero order in O_2, and negative first order in H_2O. Results are presented in Table 1 along with a comparison of results from a Pd black sample and literature values on ZrO_2-supported Pd catalyst. The rates measured on a Pd black sample, in which the sample PdO surface area was calculated by the BET method, also showed a rate comparable to the ones measured on supported samples.

The dependence of rates with temperature is shown as an Arrhenius plot in Fig. 3. The apparent activation energy measured was 125 kJ mol^{-1}; note that the rates in this plot are reported for the same concentration of products and reactants.

3.3. Characterization of the Foil before and after Reaction

The state of the foil surface was examined before and after reaction by Auger electron spectroscopy (AES), X-ray photoelectron spectroscopy (XPS), and temperature-programmed desorption (TPD). Before reaction, only features corresponding to metallic Pd can be observed by

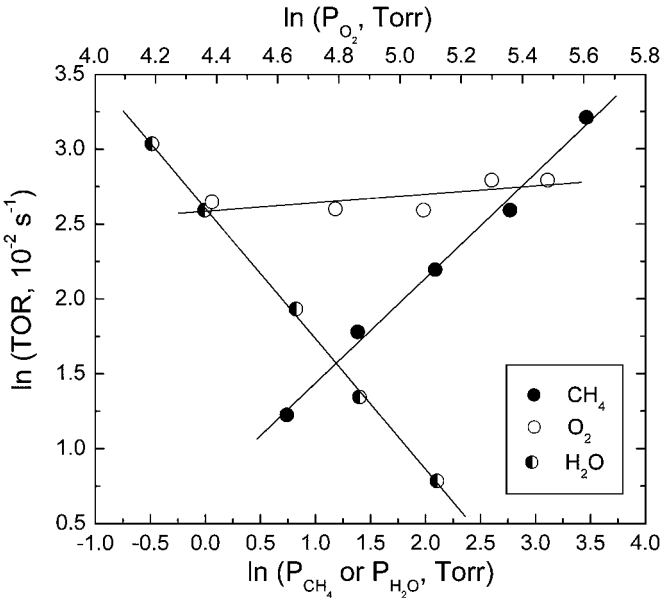

FIG. 2. Reaction order dependence for Pd foil on methane (2–32 Torr CH_4, 160 Torr O_2, N_2 to balance 800 Torr), oxygen (80–240 Torr O_2, 16 Torr CH_4, N_2 to balance 800 Torr), and water (0.5–8 Torr H_2O, 16 Torr CH_4, 160 Torr O_2, N_2 to balance 800 Torr).

AES (Fig. 4) and XPS (Fig. 5). Auger spectra show the palladium signature of a clean foil characterized by peaks at 43, 73, 78, 243, 279, and 330 eV (Fig. 4a). The AES spectrum after reaction (Fig. 4b) reveals two additional peaks at 490

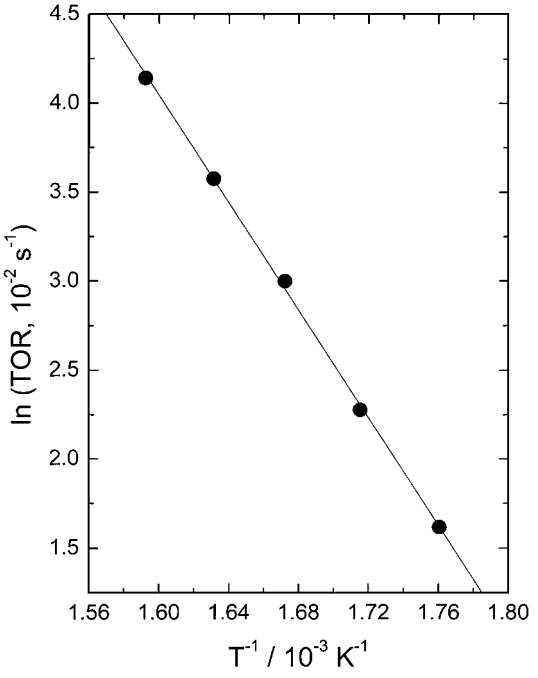

FIG. 3. Arrhenius plot for the combustion of CH_4 over Pd foil at 16 Torr CH_4, 160 Torr O_2, 1 Torr H_2O, and N_2 balance to 800 Torr. The apparent activation energy was 125 kJ mol^{-1}.

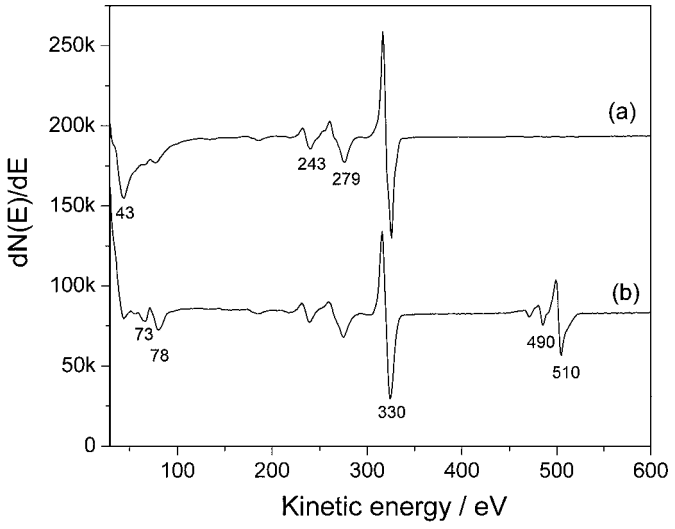

FIG. 4. AES spectra for Pd foil with characteristic peak energies: (a) clean foil and (b) after CH_4 combustion for 170 min at 598 K, 16 Torr CH_4, 160 Torr O_2, and N_2 balance to 800 Torr.

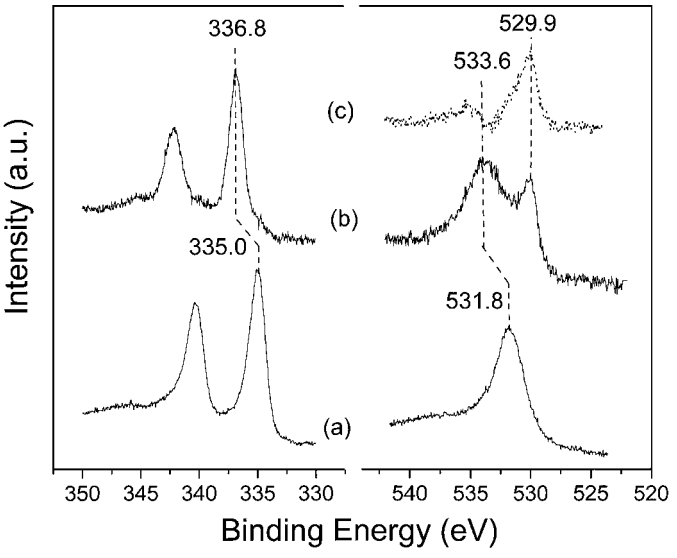

FIG. 6. XPS Pd and O spectra for Pd foil: (a) clean foil, (b) after CH_4 combustion for 170 min at 598 K, 16 Torr CH_4, 160 Torr O_2, and N_2 balance to 800 Torr, and (c) difference spectrum obtained by subtraction of Pd contribution.

and 510 eV characteristic of oxygen, which indicate the existence of an oxide layer on the foil surface with an O/Pd ratio of 0.7. The lower than 1.0 value may be due to electron beam damage to the oxide, which decomposes the oxide followed by desorption of O_2 (27). The amount of carbon could not be measured accurately by AES because of interference with the Pd peak at 279 eV. In the XPS survey spectra before reaction only the core levels of metallic palladium and its Auger electron signal are observed (Fig. 5a). After reaction, the palladium and carbon core levels plus oxygen Auger electrons are observed in the XPS survey spectrum (Fig. 5b). Figure 6 shows X-ray photoelectron spectra of the Pd 3*d* and Pd $3p_{3/2}$/O 1*s* regions taken from a clean palladium foil (spectrum a) and from a Pd foil after treatment under reaction conditions (spectrum b). The clean Pd foil is characterized by the Pd $3d_{5/2}$ and Pd $3p_{3/2}$ peaks at 335.0 and 531.8 eV. The peak position is in good agreement with those in the literature (28–31). After treatment under reaction conditions, the Pd $3d_{5/2}$ and Pd $3p_{3/2}$ peaks shifted to a higher binding energy by *ca.* 1.8 eV with new positions at 336.8 and 533.6 eV, characteristic of PdO (28, 31–35). After reaction, an O 1*s* peak at 529.9 eV characteristic of PdO appeared as well (28, 32, 33). Thus, the characteristic chemical shift of 1.8 eV observed for the Pd $3d_{5/2}$ peak, which shows no peak broadening, and the appearance of the O 1*s* peak at the appropriate energy indicate that the main chemical compound on the surface of foil after exposure to a reaction mixture is PdO. Table 2 shows the quantitative results for the XPS analysis. The atomic concentrations of the chemical elements in the near-surface region were estimated after the subtraction of a linear-type background,

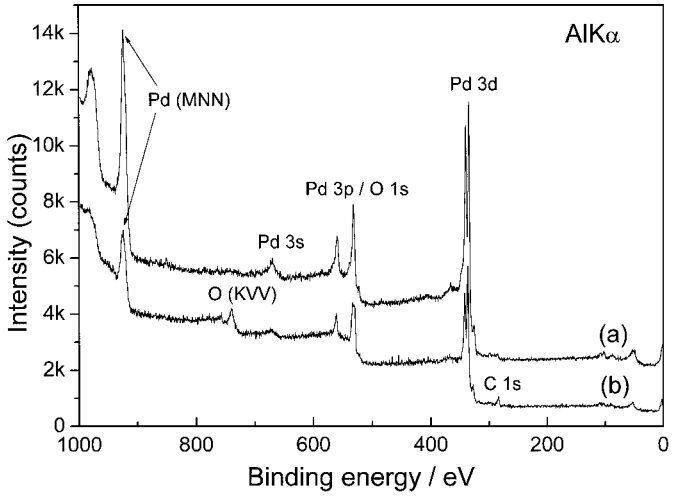

FIG. 5. XPS survey spectra for Pd foil: (a) clean foil and (b) after CH_4 combustion for 170 min at 598 K, 16 Torr CH_4, 160 Torr O_2, and N_2 balance to 800 Torr.

TABLE 2

XPS Data for Pd Foil

	Binding energy (eV)			Atomic concentration %		
Sample	Pd 3*d*	O 1*s*	C 1*s*	[Pd]	[O]	[C]
Clean foil	335.0	—	—	1.00	—	—
Foil after reaction[a]	336.8	529.9	284.5	0.32	0.37	0.32[b]

[a] Reaction at 598 K, 16 Torr CH_4, 160 Torr O_2, and N_2 balance to 800 Torr.

[b] From impurity adsorbed after reaction.

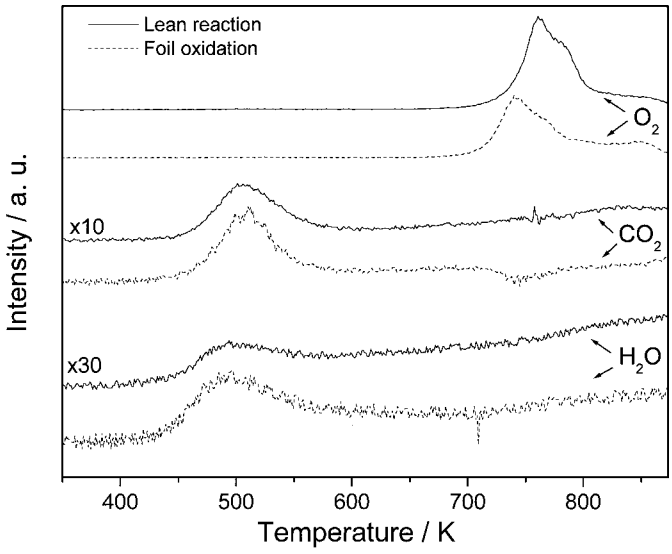

FIG. 7. TPD results after reaction combustion for 170 min at 598 K, 16 Torr CH_4, 160 Torr O_2, and N_2 balance to 800 Torr and after foil oxidation (same conditions but no methane). Foil was heated under UHV at 5 K s^{-1} up to 873 K.

taking into account the corresponding atomic sensitivity factors as described by Wagner *et al.* (29).

Temperature-programmed desorption of the foil after reaction and after oxidation (same reaction conditions but no methane) is shown in Fig. 7. The amounts of O, CO_2, and H_2O after reaction or foil oxidation were the same and corresponded to 103 layers of O, an amount of CO_2 corresponding to 13 layers of oxygen, and H_2O corresponding to 1 layer of oxygen. The XPS analysis after TPD showed a Pd 3*d* binding energy of 335.0 eV characteristic of metallic palladium. Note that no other desorption products were associated with the O_2 peak at high temperature. The CO_2 and H_2O desorption was observed at much lower temperatures, 521 K and 496 K, respectively. The presence of the same amount of CO_2 and H_2O after foil oxidation (no methane present) or reaction and the fact that the desorption temperature is lower than the reaction temperature (600 K) indicate that the carbon does not come from methane deposited during reaction. To confirm that the CO_2 measured on the TPD was not related to methane oxidation, the reaction was performed with $^{13}CH_4$. No signal from $^{13}CO_2$ could be detected, and since our sensitivity for CO_2 is 5% of a monolayer, the amount of carbon deposited after reaction has to be lower than 5% of a monolayer. An additional experiment to verify if the carbon and water observed were related to the reaction involved annealing the sample after reaction in a vacuum up to the reaction temperature (598 K) at a heating rate of 5 K s^{-1}, and then measuring the XPS spectrum. The results showed that the carbon-signal vanished, which suggests that at reaction temperature the compound responsible for CO_2 and H_2O would burn and thus carbon-containing compounds must have been deposited after reaction. A signal corresponding to metallic Pd appeared in addition to the one for PdO after this treatment, which is consistent with the use of oxygen from the PdO lattice during combustion.

An attempt to detect $Pd(OH)_2$ as a stable compound using TPD and XPS analysis was made after reaction on the Pd foil. This compound appears in the reaction mechanism in the quasi-equilibrated adsorption– desorption step that inhibits the reaction (22, 36), $2OH^* \leftrightarrow H_2O_{(g)} + O^* + *$ (where* is an adsorption site, with OH^* as the most abundant reaction intermediate). The decomposition of this compound could not be investigated directly by TPD due to the interference from the adsorbed hydrocarbon impurity discussed above which also generated a water signal. Experiments with deuterium-labeled methane will be performed in the future to address this possibility. Thermogravimetic analysis carried out by Card *et al.* (37) has shown that $Pd(OH)_2$ decomposes at about 523 K when $Pd(OH)_2$/C was heated in dry nitrogen, the same temperature range where the carbon-containing impurity burns during TPD. An upper value for the concentration of $Pd(OH)_2$, however, can be established from the XPS results. A difference spectrum in the Pd $3p_{3/2}$/O 1*s* region is shown in Fig. 6c. This spectrum was obtained after the subtraction of the Pd contribution by correction of the chemical shift for the Pd $3p_{3/2}$ peak by 1.8 eV and normalization of the intensities. The resulting spectrum represents the contribution for oxygen, with a single asymmetric peak at 529.9 eV. The absence of a pronounced peak at a binding energy higher than 529.9 eV indicates the absence of significant amounts of surface species other than PdO. Thus, the presence of $Pd(OH)_2$ would imply the appearance of an additional O 1*s* peak due to an OH group at a binding energy *ca.* 1.5 eV higher. The reference value for $Pd(OH)_2$ could not be found in the literature but the values are available for Pt and Ni compounds. The values of the O 1*s* peak reported for $Pt(OH)_4$ and for $Ni(OH)_2$ are 531.3 eV (38) and 531.2 eV (39–41), respectively. Although a quantitative estimation of the amount of $Pd(OH)_2$ on the surface could not be made, one can conclude from Fig. 6c that if present its concentration must be much less than 1-ML.

3.4. Sample Oxidation

Since there is no observable sample activation during reaction, and many reports are available to support that Pd metal is not active for the oxidation of methane at low temperatures (10, 42), the rate of surface oxidation from Pd to PdO must be fast compared to the rate of reaction. Also, if the surface area is increased due to sample oxidation it must happen at an early stage of reaction; otherwise, a sample activation would have been observed. Indeed, as shown in Fig. 8, the rate of oxidation is fast compared

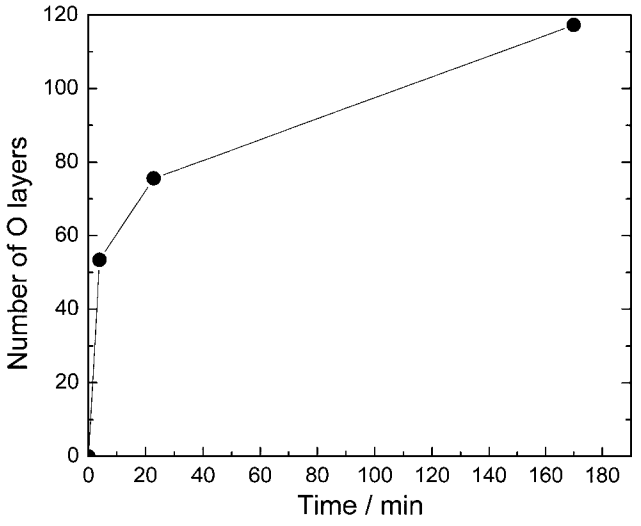

FIG. 8. Number of oxygen layers as a function of time for a Pd foil under reaction conditions 598 K, 16 Torr CH_4, 160 Torr O_2, and N_2 balance to 800 Torr.

with the rate of reaction, with 55 layers of PdO formed after 3 min. The rate of foil oxidation is a function of the time of reaction, being rapid in the early stages but decreasing as the thickness of the oxide layer increases (Fig. 8). The number of layers formed does not vary as the 1/2 power of the time, which suggests that diffusion-controlled growth is not the only phenomenon taking place during the oxidation of Pd foil under reaction conditions. For a diffusion-controlled growth of the oxide film, a parabolic law describes the oxide-film thickness growth: $L(t) \propto t^{1/2}$ (43). Electronic and oxygen anion transports developed with the Cabrera–Mott theory in combination with bulk diffusion of uncharged particles better describe the oxidation process on palladium catalysts (11).

3.5. Measurement of PdO Surface Area

For the calculation of turnover rates, the PdO surface area under reaction conditions was calculated from the geometric Pd metallic surface area assuming an average Pd surface atom density for a polycrystalline foil of 1.27×10^{15} atoms/cm^2 (44). However, the addition of oxygen to Pd to form PdO will cause the Pd structure to change from a face-centered cubic structure (characteristic lengths $a = b = c = 0.38903$ nm) to PdO which is tetragonal (characteristic lengths $a = b = 0.3036$ nm; $c = 0.534$ nm) (45). A simple calculation shows that the Pd atom density for the oxide is 60% of the density for the metal structure, indicating an overall structure expansion upon oxidation which may cause a roughened oxide surface to form.

The PdO surface area was measured by a surface exchange experiment with labeled oxygen (^{18}O isotope). The exchange experiment consisted of exposing the oxidized foil to 5 Torr $^{18}O_2$ at 598 K for 12 s into the reactor cell. These conditions are designed to ensure that the exchange between ^{16}O in PdO and ^{18}O isotope in the gas phase may happen only on the surface, without appreciable diffusion to the bulk. In fact, the number of layers exchanged under these conditions calculated from Fig. 8 is around one and the rate of recombination of O atoms at the surface of PdO calculated from the results of Au-Yeung *et al.* (46) is about 4 s^{-1}. Thus, only surface oxygen should be exchanged. The amount of ^{18}O exchanged was measured in a TPD experiment by quantifying all the desorbed compounds containing ^{18}O. The reference point for oxygen coverage was made by assuming that a foil exposed to O_2 at room temperature will form an oxygen layer with 0.25 ML coverage at saturation. This coverage is well established for a Pd(111) single crystal (25, 26) and since a foil is composed of mostly (111) planes, the 0.25 ML coverage should be a good approximation. The PdO surface after reaction under excess oxygen was 2.2 cm^2, based on the measured geometric surface area (1.0 cm^2) of the foil.

It is important to note that the surface area did not appear to change after consecutive reactions or after the sample was cooled from reaction temperature. This was inferred by carrying out consecutive reaction experiments with the sample cooled after reaction and a new charge introduced into the reactor. The rates were the same on consecutive experiments within experimental error. However, cooling the sample after reaction under certain conditions (after treatment in excess methane) may change the surface area as detailed by Monteiro *et al.* (47).

4. DISCUSSION

4.1. Reaction Orders

The reaction orders measured for CH_4, O_2, and H_2O are similar to the ones for supported catalysts (Table 1) (20–23). The CO_2 order dependence, which is proportional to $[CO_2]^{-2}$ when the concentration of CO_2 is higher than the concentration of H_2O (20), was not measured since the conditions of this work were outside the range where CO_2 would inhibit rates.

4.2. Structure Sensitivity and Turnover Rates

The dependence of the particular arrangement of PdO crystal planes on the turnover rates is an issue not yet settled. The answer to this question will have to wait until rate measurements on well-defined PdO single crystal surfaces are made. Combustion of methane in excess oxygen over Pd-based catalysts at low temperatures (<600 K) has been described as a structure-sensitive reaction by some authors (6, 8, 48–50) and as insensitive by others (9, 20, 51). Higher rates are reported for larger Pd particles (22). The steady-state turnover rate of 59×10^{-2} s^{-1} for a Pd foil in this work is about 3 times higher than the highest turnover rate reported on supported

catalysts (Table 1). This result shows that the value obtained for the foil is an upper limit for the CH_4 combustion rate on PdO on supported catalysts under lean conditions (excess oxygen). However, one should still consider the following possibilities: (1) the particle size is maximized on the foil and as suggested most recently by Fujimoto *et al*. (22) this would be the reason for the higher rate; (2) there is a detrimental effect from the support on PdO as shown by Rodriguez *et al*. (52) and the foil would be free from it; (3) crystalline PdO is more reactive than the amorphous one (10, 11) and the foil may preferentially form one of them (we do not know which form the foil is in); and (4) there is a substantial increase in the PdO surface area on the foil. Concerning the latter argument, the PdO surface area changes by a factor of only 2, which is not a significant change.

The fact that the turnover rate is only a factor of 3 higher than the highest turnover rate reported on supported catalysts (Table 1) is an indication that the reaction may not be sensitive to the structure of the oxide. As shown by Fujimoto *et al*. (22), the turnover rate variation with the particle size in the range 1–10 nm is only a factor of 3. The factor of 3 difference in this case is not significant in view of the fact that the turnover rate needs to be calculated per unit of PdO surface area but the comparisons are based on the Pd metal surface area. This issue will be discussed next.

4.3. Measurement of PdO Surface Area

On supported Pd catalysts, the measurement of Pd surface area is based on the adsorption of probe molecules H_2 or CO on metallic Pd, thus requiring the sample to be reduced (usually in H_2) before chemisorption. However, PdO is the active phase and the incorporation of oxygen due to the oxidation process in the lattice of metallic palladium is associated with volume changes and thus it may create a surface with porosity or with sufficient roughness to increase substantilly the geometric surface area. The error in surface area measurement caused by reduction of PdO on supported samples is probably a function of particle size, with small particles showing no effect upon reduction since most of the atoms will be on the surface and the large particles, possibly showing large differences. This may explain why some results in the literature show a modest but distinct variation of rate with particle size (22). This increase in area by oxidation will be maximum for a foil since the potential for the formation of a porous and roughened structure is greatest.

We propose that isotope exchange with $^{18}O_2$ could also be used in the measurement of surface areas of supported samples. A direct comparison of rates on foils with the ones on supported catalysts will have to wait untill the PdO surface area can be measured for these samples.

A Pd black sample was also used to estimate the actual PdO surface area. The PdO surface area was measured by the BET method (47 $m^2\ g^{-1}$) after reaction. The turnover rate based on the PdO surface area was $5 \times 10^{-2}\ s^{-1}$ at standard conditions (1 Torr H_2O, 550 K, 16 Torr CH_4, and 160 Torr O_2), a value comparable to the turnover rate based on the PdO surface area for the foil ($22 \times 10^{-2}\ s^{-1}$). The lower rates on Pd black may be the result of the migration of impurities from the bulk of Pd black to the surface, a possibility we could not test.

The fact that the surface area of the foil increases after reaction is an indication that the same may be true for supported samples. The increase in surface area by a factor of 2 on a foil may also be the upper limit of surface area variation on supported samples unless a different mechanism, such as spreading of the oxide on the support (53, 54), is important for supported samples. Ribeiro *et al.* (20) have shown an increase in measured Pd surface area on supported samples by 3.2-fold after the metallic sample is oxidized to PdO. As an added complication, despite the increase in the surface area attributed to the spreading of PdO onto the support surface, the comparison of the per gram rate for methane oxidation showed no change. These results have convinced the authors that PdO layer spread onto the support surface is not active. Datye *et al.* (24) have reported that in the process of PdO reformation after a high-temperature PdO $\rightarrow$ Pd transformation on 5% Pd/θ-Al_2O_3 catalyst, the oxidation of large Pd particles (>20 nm) led to formation of polycrystalline PdO with the roughening of the particle surfaces. The activity, expressed in terms of degree of conversion, of this rough PdO was higher than that seen on annealed PdO for the CH_4 combustion.

4.4. Sample Oxidation

The straight line obtained in Fig. 1b extrapolates to zero, suggesting that although the sample is constantly being oxidized under our reaction conditions (Fig. 8), the surface area increase must happen at a very early stage of reaction and then stop; otherwise, the rate would have increased with time. That the surface area increase may happen at an early stage of reaction is corroborated by the fact that about 55 layers of PdO are formed after only 3 min of reaction at 598 K (Fig. 8). This fact suggests that Pd catalysts should oxidize readily under our reaction conditions (excess oxygen, about 600 K) and should not show an activation effect due to oxidation. Activation effects on supported samples must not be caused by Pd oxidation.

4.5. Sample Activation

Activation periods have been reported on supported Pd catalysts. Some hypotheses have been raised to explain such time-dependent behavior, such as the presence of impurities (6, 9, 14, 16–18, 48, 51), support interaction (52, 55), sample oxidation state (10, 42), high-temperature treatment (>800°C) in O_2 (56), or formation of an inactive oxide

phase that inhibits oxidation (24, 57). Impurities left on the catalyst surface by precursor salts (e.g., chlorine) can interact with the catalytic sites, but the water produced in the reaction removes them, contributing to an increase in the activity as a function of time. Since PdO is the active phase for CH_4 combustion, its formation is required when reduced samples are used. A slow PdO formation rate due to a strong metal–support interaction can affect the reactivity. Thus, fresh samples would not be fully activated at the beginning of the reaction and an activation period would be observed. In contrast to this behavior, Pd foils did not show any activation period in our work. However, steady-state activity was not reached easily when impurities were present. Starting with a fresh foil, sulfur was the most abundant contaminant and the initial cleaning process (sputtering/O_2 exposure/annealing) was sufficient to remove it. Sulfur elimination did not produce a fully activated catalyst, however. Turnover rates in the initial runs were low and sample deactivation took place. Analysis by XPS showed the presence of phosphorous and silica on the surface every time the samples deactivated. Such impurities were not detected before reaction which suggests that sample exposure to the high-pressure reaction conditions caused the impurities to migrate from the bulk to the surface. Thus, for the Pd foil to reach its highest and constant activity, the sample was exposed to reaction conditions followed by the usual cleaning procedure under UHV conditions. These cycles of reaction–cleaning were performed until the sample reached the maximum steady-state rate and no impurities were detected by XPS.

To speed up the cleaning process, a palladium foil underwent a special pretreatment before being mounted in the sample holder. The objective was to bring to the surface all impurities in the bulk phase, so the number of cycles to clean the foil would be reduced. The pretreatment consisted of flowing a lean mixture (2% CH_4, 20% O_2, and He balance to atmospheric pressure) at a rate of 40 $cm^3\ min^{-1}$, 773 K for 15 h, followed by sample heating at 973 K for 15 min under helium flow. After the pretreatment, the sample was submitted to the initial cleaning process (sputtering/O_2 exposure/annealing), which removed surface impurities followed by a reaction rate measurement. The initial turnover rate was about $29 \times 10^{-2}\ s^{-1}$, a value higher than that on the initial runs with no pretreatment (around $6 \times 10^{-2}\ s^{-1}$), but the sample still deactivated due to impurities migrating to the surface.

An important question is whether Pd foils were solely being cleaned or whether some activation also took place. Is it possible that as the impurities are being removed the surface finds a better arrangement that increases its catalytic activity? The answer seems to be no, since the samples are sputtered clean and annealed after each reaction, a process that would destroy any special structural arrangement on the surface. Descorme *et al.* (58) in the kinetic studies of catalytic combustion of ethane over Pd foils reported that to prepare a stable catalyst with maximum activity, preactivation of the foil by reaction at 723 K under fuel-rich conditions was necessary, even though the samples were sputtered and annealed after the treatment. Two or more treatments were needed for the reaction rate to become invariant and the difference in activity between fresh and activated foils was about a factor of 20. We postulate that these treatments were effective because we have observed that under excess methane the surface uptake of oxygen is a factor of 3–4 higher than after reaction in excess oxygen, which facilitates the bulk impurities' migration to the surface and subsequent elimination by sputtering (47).

Baldwin and Burch (18) reported the activation of supported palladium catalysts under reaction conditions and assigned the increase of activity to structural changes, created by carbon dissolution into the bulk of palladium. Some carbon dissolved in the palladium lattice would account for a change in morphology leading to more active catalysts. In our studies, temperature-programmed desorption results on palladium foil after reaction in excess oxygen did not show any evidence of carbon dissolution. The PdO decomposition at temperatures higher than 700 K released only oxygen and no carbon-related compound desorption was observed. Isotope labeling of methane ($^{13}CH_4$) showed that low-temperature $^{13}CO_2$ does not come from carbon species deposited under our reaction conditions. In fact, even carbon-containing impurities are completely burned on the surface of the foil even under UHV conditions at a temperature lower than the standard reaction temperature. At the higher temperature and partial pressure of O_2 present during the reaction, any carbon compounds would be completely burned. Thus, if restructuring of the catalytic surface is occurring in the Pd foil, the cause cannot be related to carbon dissolution.

4.6. Surface Species

The surface species present after reaction were probed using TPD, XPS, and AES. The main species observed were oxygen and palladium. No metallic Pd could be found after reaction. The CO_2 and H_2O peaks on the TPD were due to an impurity adsorbed on the surface after reaction. The same impurity gives a carbon signal in the XPS. Blank experiment (only oxygen present) and experiments with labeled molecules described above confirmed that the carbon signal comes from the impurity. The presence of $Pd(OH)_2$ can be excluded unless its concentration is much less than 1 ML.

5. SUMMARY

The complete oxidation of methane under excess oxygen was studied over a Pd foil at 598 K. The kinetic behavior was consistent with the one observed for supported Pd catalysts, showing similar reaction orders with a rate expression $r = k[CH_4]^{0.7}[O_2]^{0.2}[H_2O]^{-0.9}$.

There were no activation periods for the Pd foil samples. However, steady-state turnover rates were reached only after the elimination of impurities (S, P, and Si) in the foil. To reach a high and invariant activity, the samples were exposed to reaction conditions many times followed by Ar sputtering. On clean foils, the steady-state turnover rate is 59×10^{-2} s^{-1} at 550 K, 160 Torr O_2, 16 Torr CH_4, 1 Torr H_2O, and N_2 balance to 800 Torr with the number of sites equal to the number of Pd atoms based on the Pd geometric surface area. This rate is 3 times higher than the highest rate reported for supported Pd catalysts. This value is regarded as a nominal turnover rate because its calculation was based on the geometric surface area of the foil, not the PdO surface area. This value can be compared with the turnover rates reported for supported particles, since they were also based on the metallic surface area.

Under our reaction conditions, 55 layers of the oxide are formed during the first 3 min of reaction, which indicates that palladium oxide (PdO) is the active phase. Palladium needs to expand its structure in order to accommodate the oxygen and for this reason a surface roughening and change in surface area may happen. Thus, the turnover rate calculations based on the number of Pd sites counted in the reduced state of the catalyst may be an overestimation of the actual turnover rate. To overcome this problem, the PdO surface area was measured by a surface exchange experiment using $^{18}O_2$ isotope exchange. The amount of ^{18}O exchanged with the surface was measured in a TPD experiment. The results showed an increase by a factor of 2 in the Pd foil surface area after the foil oxidation. The turnover rate was recalculated on the basis of the estimated PdO surface area, with a new value of 22×10^{-2} s^{-1}, at 550 K, 160 Torr O_2, 16 Torr CH_4, 1 Torr H_2O, and N_2 balance to 800 Torr which is 2 times lower than the nominal one.

ACKNOWLEDGMENTS

We gratefully acknowledge support from the Office of Heavy Vehicle Technologies, U.S. Department of Energy, and the Office of Basic Energy Sciences, Chemical Sciences, U.S. Department of Energy, Grant DE-FG02-00ER15026.

REFERENCES

1. Dalla Betta, R. A., and Rostrup-Nielsen, T., *Catal. Today* **47**, 369 (1999).
2. Anderson, R. B., Stein, K. C., Feenan, J. J., and Hofer, L. J. E., *Ind. Eng. Chem.* **53**, 809 (1961).
3. Cusumano, J. A., *CHEMTECH* **22**, 482 (1992).
4. Bayer, G., and Wiedemann, H. G., *Thermochim. Acta* **11**, 79 (1975).
5. Mallika, C., Sreedharan, O. M., and Gnanamoorthy, J. B., and *J. Less-Common Met.* **95**, 213 (1983).
6. Hicks, R. F., Qi, H., Young, M. L., and Lee, R. G., *J. Catal.* **122**, 280 (1990).
7. Muller, C. A., Maciejewski, M., Koeppel, R. A., Tschan, R., and Baiker, A., *J. Phys. Chem.* **100**, 20006 (1996).
8. Muller, C. A., Maciejewski, M., Koeppel, R. A., and Baiker, A., *J. Catal.* **166**, 36 (1997).
9. Baldwin, T. R., and Burch, R., *Appl.Catal.* **66**, 359 (1990).
10. Carstens, J. N., Su, S. C., and Bell, A. T., *J. Catal.* **176**, 136 (1998).
11. Su, S. C., Carstens, J. N., and Bell, A. T., *J. Catal.* **176**, 125 (1998).
12. Koning, D., Weber, W. H., Poindexter, B. D., McBride, J. R., Graham, G. W., and Otto, K., *J. Catal. Lett.* **29**, 329 (1994).
13. Graham, G. W., Konig, D., Poindexter, B. D., Remillard, J. T., and Weber, W. H., *Top. Catal.* **8**, 35 (1999).
14. Simone, D. O., Kennelly, T., Brungard, N. L., and Farrauto, R. J., *Appl. Catal.* **70**, 87 (1991).
15. Peri, S. S., and Lund, C. R. F., *J. Catal.* **152**, 410 (1995).
16. Garbowski, E., Feumi-Jantou, C., Mouaddib, N., and Primet, M., *Appl. Catal. A: Gen.* **109**, 277 (1994).
17. Garbowski, E., and Primet, M., *Appl. Catal. A: Gen.* **125**, 185 (1995).
18. Baldwin, T. R., and Burch, R., *Catal. Lett.* **6**, 131 (1990).
19. Somorjai, G. A., *J. Phys. Chem. B* **104**, 2969 (2000).
20. Ribeiro, F. H., Chow, M., and Dalla Betta, R. A., and *J. Catal.* **146**, 537 (1994).
21. Burch, R., Urbano, F. J., and Loader P. K., *Appl. Catal. A: Gen.* **123**, 173 (1995).
22. Fujimoto, K.-I., Ribeiro, F. H., Avalos-Borja, M., and Iglesia, E., *J. Catal.* **179**, 431 (1998).
23. van Giezen, J. C., van den Berg, F. R., Kleinen, J. L., van Dillen, A. J., and Geus, J. W., *Catal. Today* **47**, 287 (1999).
24. Datye, A. K., Bravo, J., Nelson, T. R., Atanasova, P., Lyubovsky, M., and Pfefferle, L., *Appl. Catal. A: Gen.* **198**, 179 (2000).
25. Conrad, H., Ertl, G., Kueppers, J., and Latta, E. E., *Surf. Sci.* **65**, 245 (1977).
26. Zheng, G., and Altman, E. I., *Surf. Sci.* **462**, 151 (2000).
27. Voogt, E. H., Mens, A. J. M., Gijzeman, O. L. J., and Geus, J. W., *Surf. Sci.* **373**, 210 (1997).
28. Kim, K. S., Gossmann, A. F., and Winograd, N., *Anal. Chem.* **46**, 197 (1974).
29. Wagner, C. D., Riggs, W. M., Davis, L. E., Moulder, J. F., and Muilenberg, G. E., "Handbook of X-Ray Photoelectron Spectroscopy." Perkin-Elmer Corp., Eden Prairie, MN, 1978.
30. Nyholm, R., and Martensson, N., *J. Phys. C* **13**, L279 (1980).
31. Haack, L. P., and Otto, K., *Catal. Lett.* **34**, 31 (1995).
32. Peuckert, M., *J. Phys. Chem.* **89**, 2481 (1985).
33. Tressaud, A., Khairoun, S., Tohara, H., and Watanabe, N., *Z. Anorg. Allg. Chem.* **540–541**, 291 (1986).
34. Tura, J. M., Regull, P., Victori, L., and Dolors de Castella, M., *SIA, Surf. Interface Anal.* **11**, 447 (1988).
35. Shyu, J. Z., Otto, K., Watkins, W. L. H., Graham, G. W., Belitz, R. K., and Gandhi, H. S., *J. Catal.* **114**, 23 (1988).
36. Au-Yeung, J., Chen, K., Bell, A. T., and Iglesia, E., *J. Catal.* **188**, 132 (1999).
37. Card, R. J., Schmitt, J. L., and Simpson, J. M., *J. Catal.* **79**, 13 (1983).
38. Peuckert, M., Coenen, F. P., and Bonzel, H. P., *Electrochim. Acta* **29**, 1305 (1984).
39. McIntyre, N. S., and Cook, M. G., *Anal. Chem.* **47**, 2208 (1975).
40. Dickinson, T., Povey, A. F., and Sherwood, P. M. A., *J. Chem. Soc., Faraday Trans. 1* **73**, 327 (1977).
41. Loechel, B. P., and Strehblow, H. H., *J. Electrochem. Soc.* **131**, 713 (1984).
42. Burch, R., and Urbano, F. J., *Appl. Catal. A: Gen.* **124**, 121 (1995).
43. Fromhold, J., A. T., *in "Theory of Metal Oxidation"* (S. Amelinckx, R. Gevers, and J. Nihoul, Eds.), Defects in Crystalline Solids, Vol. 1. North-Holland, New York, 1976.
44. Anderson, J. R., *in* "Structure of Metallic Catalysts," p. 296. Academic Press, New York, 1975.
45. Samsonov, G. V., *in* "The Oxide Handbook." IFI/Plenum Data Corp., New York, 1973.
46. Au-Yeung, J., Bell, A. T., and Iglesia, E., *J. Catal.* **185**, 213 (1999).
47. Monteiro, R. S., Zemlyanov, D., Storey, J. M., and Ribeiro, F. H., submitted for publication (2001).

48. Hicks, R. F., Qi, H., Young, M. L., and Lee, R. G., *J. Catal.* **122**, 295 (1990).
49. Muller, C. A., Maciejewski, M., Koeppel, R. A., and Baiker, A., *Catal. Today* **47**, 245 (1999).
50. Lyubovsky, M., Pfefferle L., Datye, A., Bravo, J., and Nelson, T., *J. Catal.* **187**, 275 (1999).
51. Baldwin, T. R., and Burch, R., *Appl. Catal.* **66**, 337 (1990).
52. Rodriguez, N. M., Oh, S. G., Betta, R. A., and Baker, R. T. K., *J. Catal.* **157**, 676 (1995).
53. Chen, J. J., and Ruckenstein, E., *J. Phys. Chem*. **85**, 1606 (1981).
54. Lieske, H., and Völter, J., *J. Phys. Chem*. **89**, 1841 (1985).
55. Farrauto, R. J., Lampert, J. K., Hobson, M. C., and Waterman, E. M., *Appl. Catal. B* **6**, 263 (1995).
56. Lyubovsky, M., and Pfefferle, L., *Appl. Catal. A: Gen*. **173**, 107 (1998).
57. McCarty, J. G., *J. Catal. Today* **26**, 283 (1995).
58. Descorme, C., Jacobs, P. W., and Somorjai, G. A., *J. Catal.* **178**, 668 (1998).